UCLA
UCLA Previously Published Works

Title

Clinical and radiographic delineation of Bent Bone Dysplasia-FGFR2 type or Bent Bone Dysplasia with Distinctive Clavicles and Angel-shaped Phalanges

Permalink

https://escholarship.org/uc/item/91w3v7fx

Journal

American Journal of Medical Genetics Part A, 170(10)

ISSN

1552-4825

Authors

Krakow, Deborah
Cohn, Daniel H
Wilcox, William R
et al.

Publication Date

2016-10-01

DOI

10.1002/ajmg.a.37772

Peer reviewed

Clinical and Radiographic Delineation of Bent Bone Dysplasia-FGFR2 Type or Bent Bone Dysplasia with Distinctive Clavicles and Angel-Shaped Phalanges

Deborah Krakow[1,2,3,4,*], Daniel H. Cohn[1,4,5], William R. Wilcox[4,6], Grace J. Noh[7], Leslie J. Raffel[7], Anna Sarukhanov[1], Margarita H. Ivanova[1], Moise Danielpour[8], Dorothy K. Grange[9], Alison M. Elliott[10], Jonathan A. Bernstein[11], David L. Rimoin[†], Amy E. Merrill[12], and Ralph S. Lachman[4,13]

[1]Department of Orthopaedic Surgery, University of California, Los Angeles, California

[2]Department of Human Genetics, University of California, Los Angeles, California

[3]Department of Obstetrics and Gynecology, University of California, Los Angeles, California

[4]International Skeletal Dysplasia Registry, University of California, Los Angeles, California

[5]Department of Molecular Cell and Developmental Biology, University of California, Los Angeles, California

[6]Department of Human Genetics, Emory University School of Medicine, Atlanta, Georgia

[7]Department of Pediatrics, Cedars-Sinai Medical Center, Los Angeles, California

[8]Department of Surgery, Cedars-Sinai Medical Center, Los Angeles, California

[9]Division of Genetics and Genomic Medicine, Department of Pediatrics, Washington University School of Medicine, Saint Louis, Missouri

[10]Department of Medical Genetics, University of British Columbia, Vancouver, British Columbia

[11]Department of Pediatrics, Stanford University School of Medicine, Stanford, California

[12]Center for Craniofacial Molecular Biology-Ostrow School of Dentistry, Keck School of Medicine, University of Southern California, Los Angeles, California

[13]Department of Radiology, Stanford University School of Medicine, Stanford, California

Abstract

Bent Bone Dysplasia-FGFR2 type is a relatively recently described bent bone phenotype with diagnostic clinical, radiographic, and molecular characteristics. Here we report on 11 individuals, including the original four patients plus seven new individuals with three longer-term survivors. The prenatal phenotype included stillbirth, bending of the femora, and a high incidence of

[*]Correspondence to: Deborah Krakow, M.D., David Geffen School of Medicine at UCLA, BSRB/OHRC, 615 Charles E. Young Drive S, Room 410, Los Angeles, CA 90095. dkrakow@mednet.ucla.edu.
[†]In memoriam.
Festschrift honoring John C. Carey

polyhydramnios, prematurity, and perinatal death in three of 11 patients in the series. The survivors presented with characteristic radiographic findings that were observed among those with lethality, including bent bones, distinctive (moustache-shaped) small clavicles, angel-shaped metacarpals and phalanges, poor mineralization of the calvarium, and craniosynostosis. Craniofacial abnormalities, hirsutism, hepatic abnormalities, and genitourinary abnormalities were noted as well. Longer-term survivors all needed ventilator support. Heterozygosity for mutations in the gene that encodes Fibroblast Growth Factor Receptor 2 (*FGFR2*) was identified in the nine individuals with available DNA. Description of these patients expands the prenatal and post-natal findings of Bent Bone Dysplasia–FGFR2 type and adds to the phenotypic spectrum among all *FGFR2* disorders.

Keywords

skeletal dysplasia; FGFR2; craniosynostosis; bent bone dysplasia

INTRODUCTION

Fibroblast growth factor (FGF) signaling is mediated through FGF receptor tyrosine kinases (FGFR1-4). The binding of FGF ligand to FGF receptors (FGFR) is mediated in part by heparan sulfate glycosaminoglycans, induces receptor dimerization and tyrosine transphosphorylation of the activation loop. Once FGFR is in the active conformation, adaptor proteins, and other signaling molecules are recruited to propagate signals through multiple transduction cascades that facilitate numerous processes involved in development and tissue homeostasis.

Heterozygous mutations in *FGFR2* have been identified in a wide spectrum of bone, skin, and cancer pathologies. The *FGFR2*-related skeletal disorders vary widely in clinical presentation, each with its distinct radiographic and clinical findings. Heterozygosity for mutations in *FGFR2* has been found in Apert (MIM 101200), craniosynostosis with cutis gyrata (Beare-Stevenson, MIM 123790), Pfeiffer (MIM 101600), Jackson-Weiss (MIM 123150), Antley-Bixler (MIM 207410), and Crouzon (MIM 123500) syndromes [Moosa and Wollnik, 2015]. While these autosomal dominant disorders share the common feature of craniosynostosis, other facial and skeletal abnormalities, particularly affecting the hands and feet, show varied involvement. The vast majority of *FGFR2* mutations in these craniosynostosis disorders are generally considered to have a "gain-of-function mechanism," as they are largely localized in the immunoglobulin-like IIIa and IIIc loops in the extracellular ligand-binding domain of the receptor and lead to enhanced ligand affinity, ligand-binding promiscuity, or ligand-independent activation [Hatch, 2010]. Conversely, mutations within the tyrosine kinase domain of FGFR2 that diminish receptor activity cause Lacrimo-Auriculo-Dento-Digital (LADD syndrome, MIM 149730). Patients with LADD syndrome present with underdeveloped lacrimal and salivary glands, hearing loss, peg-shaped teeth, and facial dysmorphism [Rohmann et al., 2006; Shams et al., 2007]. Skeletal abnormalities in LADD syndrome include short ulnae and radii, radio-ulnar fusions, and variably penetrant digital features of the hand including fifth finger clinodactyly, duplication

of the distal phalanx of the thumb, triphalangeal thumb, and cutaneous syndactyly [Hollister et al., 1974].

The most recent addition to the *FGFR2* spectrum of disorders is Bent Bone Dysplasia-FGFR2 type, also known as Bent Bone Dysplasia with Distinctive (Moustache) Clavicles and Angel-shaped Phalanges. Radiographic and clinical findings have firmly established this disorder as a distinct dominant *FGFR2* disorder [Merrill et al., 2012; Scott et al., 2014; Handa et al., 2016; Stichelbout et al., 2016]. This unique disorder results from FGFR2 dysfunction unlike that described in the craniosynostosis syndromes or LADD syndrome. Instead, the bent bone dysplasia phenotype results from missense mutations that introduce amino acids with charged side-chains into the hydrophobic transmembrane domain of FGFR2. Subsequently, ligand-induced FGFR2 signaling at the cell surface is reduced and the intracellular functions for the receptor in the nucleus are enhanced [Merrill et al., 2012; Neben and Merrill, 2015].

In this study, we describe 11 individuals with this disorder, including the four previously published patients and seven newly described individuals that include three longer-term survivors. In addition to our cohort, three other patients with similar radiographic findings have been reported, one recognized in the prenatal period [Handa et al., 2016], one in which there was a neonatal death [Stichelbout et al., 2016], and one longer-term survivor [Scott et al., 2014]. The patients in our series showed findings diagnostic for Bent Bone Dysplasia-FGFR2 type and include expanded clinical and radiographic features. Similar to other *FGFR2* disorders, phenotypic variability was noted even among individuals with identical mutations.

MATERIALS AND METHODS

Patients were recruited through the International Skeletal Dysplasia Registry under an approved human subjects protocol. Clinical information, including prenatal and postnatal clinical data and imaging studies were collected. DNA was extracted either from blood or cultured fibroblasts by established protocols (Qiagen, Carlsbad, CA). Serum Fibroblast Growth Factor 23 (FGF23) levels were measured by a commercial laboratory (Mayo Clinic Laboratories).

To confirm the diagnosis of BBD-FGFR2 type, the 17 coding exons of *FGFR2* were amplified by PCR from genomic DNA, and underwent bi-directional Sanger sequence analysis [Merrill et al., 2012]. Sequences were compared with the *FGFR2* reference sequence [NM_000141.4] using Sequencer (Gene Codes, Ann Arbor, MI).

RESULTS

Prenatal Findings

Prenatal abnormalities were noted in all affected patients. The prenatal findings are summarized in Table I. Two of the eleven individuals (International Skeletal Dysplasia Registry (ISDR) reference numbers R07-513 and R06-374) underwent termination of pregnancy for severe skeletal findings identified at 18 and 22 weeks, respectively (Table I).

In one patient an increased nuchal translucency in the first trimester was noted. Consistent ultrasound findings included small for gestational age by ultrasound parameters, short bent femora and other appendicular bones, micrognathia, acrocephaly, short umbilical cord, and frequently, polyhydramnios (4/11). For three of the 11 individuals, the fetuses delivered stillborn in the third trimester.

Postnatal and Radiographic Findings in Neonatal Survivors

In the original description of this disorder, the phenotype was uniformly lethal, but three newly described individuals survived the newborn period. One longer-term survivor (R11-114), who was heterozygous for an *FGFR2* c.1141T>G mutation that implied a p.Tyr381Asp substitution, was born prematurely at 30 weeks gestation. Polyhydramnios was noted prenatally. Apgars were 4 and 7 at 1 and 5 min, respectively. Review of delivery records noted a subjectively short umbilical cord. Birth weight was 1,500 g (50th centile), birth length 37 cm (3rd centile), and OFC 28 cm (25th–50th centile) (Table I). At birth she had blue-tinged sclera, proptosis, dysmorphic features, and bowing of all extremities with greater involvement of the lower limbs (Fig. 1) (Table I). Her neonatal course was complicated by progressive intracranial ventricular dilation requiring drainage. She developed multiple suture craniosynostosis and underwent surgery for worsening hydrocephaly and an Arnold-Chiari malformation. Neurosurgical procedures included sagittal suture release, suboccipital craniotomy, and C1 laminectomy. Post operatively she had an episode of self-extubation lasting 45 min because of difficult reintubation, with a probable anoxic injury. Laryngoscopy showed edema of the laryngeal outlet with edematous arytenoid and interarytenoid areas. During this time, tracheostomy and gastrostomy tubes (G-tube) were placed. She was noted to have bilateral medullary nephrocalcinosis without hypercalciuria.

The patient was re-evaluated at 7 months. Developmentally, she was able to sit with support. She smiled and rolled over at 4 months of age and had head control despite her relative macrocephaly. Her parents reported that one of her globes spontaneously popped out and was subsequently massaged back into place. Her parents reported episodes of vomiting and an enlarging OFC. On examination, her length was 57.2 cm (−3.5 SD), weight was 5.02 kg (−3.5 SD), and OFC was 40 cm (5th–10th centile), enlarging out of proportion to the rest of her growth. Her metopic suture was wide open with a tense fontanelle and ridging of her coronal sutures. A CT scan of the brain showed a significant increase in ventricular dilation and compression of the superior sagittal sinus, and a ventriculoperitoneal shunt was placed. At her 10-month visit, her hydrocephalus had significantly decreased. At that visit her length was 59.7 cm (−4.5 SD) and weight was 4.9 kg (−5.5 SD). Her parents noted that she was no longer able to hold her head up. She was still able to sit with support and move her arms toward objects, but without any purposeful grasp. At last contact, she was alive at 13 months of age.

The second longer-term survivor (R15-166), who was heterozygous for a c.1141T>G, mutation implying a p.Tyr381Asp substitution mutation, presented prenatally with abnormalities of the skeleton and polyhydramnios (Table I). She was delivered at 35 weeks gestation by Cesarean for breech presentation, was floppy on delivery with no respiratory

effort, and Apgars were 1, 1, and 3 at 1, 5, and 20 min. Intubation was performed at delivery and was reported as difficult. She presented with a cloverleaf-shaped skull, proptosis, and other characteristic dysmorphic features (Fig. 1). Tracheostomy was performed due to a small chest and chronic respiratory failure with hypoxia, and she was ventilator dependent. At her last evaluation at 5 months of age her height was 55.5 cm (−3 SD), weight 6.78 kg (50th centile) and OFC 45.8 cm (>90th centile). Her clinical exam showed characteristic features of BBD-FGFR2 type that included severe midface hypoplasia, a cloverleaf-shaped skull, proptosis, a protruding tongue, no organomegaly, shortening of all appendicular segments, ligamentous laxity and severe brachymetacarpia, and brachydactyly. In addition, she was globally developmentally delayed and could not roll over. At this time, serum FGF23 levels were found to be elevated at 278 RU/ml (NL = <230 RU/ml).

The features of the third longer-term survivor, R11-456, who was heterozygous for the substitution mutation c.1141T>G, mutation implying a p.Tyr381Asp substitution, are delineated in Table I. A skeletal dysplasia was suspected at the 23 week ultrasound, which showed IUGR and bent femora. Micrognathia was identified at the 27 week ultrasound. The affected male infant was delivered after spontaneous labor at 31 weeks gestation. Apgar scores were 1, 6, and 6 at 10 min. Resuscitation was difficult, the patient was intubated and epinephrine was administered.

Birth height, weight, and OFC were appropriate for gestational age. The physical exam showed a prominent glabella and forehead, a broad, depressed nasal bridge, proptosis, anteverted nares, micrognathia, a protuberant tongue, a prominent xiphoid, and hypertrichosis (Fig. 1). The patient was maintained on a high frequency oscillatory ventilator for 2 weeks and subsequently transitioned to conventional mechanical ventilation. A tracheostomy was performed at 2 weeks of age. A gastrostomy tube was placed and Nissen fundoplication performed at 2 months of age. Efforts to transition to CPAP were unsuccessful. A MRI of the brain performed at 2 months was reported as normal. At 3 months of age he was on full G-tube feeding regimen and stable on conventional ventilation. At that time his family elected palliative care and withdrawal of ventilator support. At the time of passing the patient continued to have a large anterior fontanel and widely patent metopic sutures. His head had taken on a scaphocephalic appearance as well, and his cheeks were increasingly full. Prominent infraorbital creases and micrognathia were noted.

Radiographic findings—All 11 individuals shared a distinct radiographic phenotype that included poor mineralization of the calvarium with multi-sutural craniosynostosis, midface hypoplasia, mandibular hypoplasia, small abnormal teeth (Fig. 2), small moustache-shaped clavicles (with only the medial portion present), a small bell shaped chest with wavy ribs in some patients, 11 ribs in some patients (Fig. 3), a narrowed ileum with deficient acetabular roofs, bent bones particularly involving the femora (Fig. 4), and metacarpal/phalangeal bones with unusual, irregular shaped cortical excrescences, making them appear "angel-shaped" (Fig. 5 and Table II). Thus all had the constellation of diagnostic radiographic findings of bent bones, distinctive (moustache-shaped) clavicles, and angel-shaped metacarpals and phalanges.

Molecular analyses—In the nine probands for which DNA was available, heterozygosity for a mutation in *FGFR2* was identified. In all cases, either of two *FGFR2* codons was mutated; c. 1172T>G implying that the methionine codon at 391 was mutated to arginine (p.Met391Arg) in three cases; tyrosine codon 381 was mutated to aspartic acid (p.Tyr381Asp) in six cases. For patients for which parental bloods (three of nine) were available, all mutations were apparently de novo. In all nine individuals with molecular diagnoses, a hydrophobic residue in the transmembrane domain of the protein was replaced by an amino acid containing a charged side chain.

DISCUSSION

Commonly observed prenatal findings in the 11 individuals reported here included polyhydramnios and bent femora, similar to the patient described by Stichelbout et al. [2016]. Handa et al. [2016] described an affected 21 week fetus with a protuberant abdomen, natal teeth, anterior-posterior shortening of the vertebrae, and bilateral femoral fractures. Femoral fractures occurred in one patient reported here. Shared abnormal clinical findings associated with the phenotype included a wide-open fontanel, midface hypoplasia, proptosis, hypertelorism, a short nose with a depressed nasal bridge, a protruding tongue, and micrognathia. More variable clinical findings included low set ears, natal or abnormal teeth, clitoromegaly, hypertrichosis, hepatosplenomegaly with extramedullary hematopoiesis, Arnold-Chiari malformation, and nephrocalcinosis without hypercalciuria. Other findings seen in the patient report by Stichelbout et al. [2016] including atrial septal defect, optic nerve atrophy, and auditory evoked potentials, were not observed in the patients described here.

All three longer-term survivors described here and an additional individual reported in the literature [Scott et al., 2014] had a consistent clinical and radiographic phenotype. The affected individuals developed multisutural craniosynostosis necessitating craniotomy and ventriculoperitoneal shunting to relieve increased intracranial pressure. Other complications included the need for Nissen fundoplication and tracheostomy with mechanical ventilation. Three of the four individuals showed marked delay in achieving developmental milestones, but the etiology of the developmental delay is unclear. In one of the patients, MRI done at 2 months did not show any structural abnormalities of the brain. However, it is possible that progressive multi-suture craniosynostosis and subsequent hydrocephalus contributed to neurological decline. Interestingly, brain anomalies have been described in Pfeiffer, Apert, and Beare-Stevenson syndromes, other autosomal dominant *FGFR2* disorders, in which the brain abnormalities included simplified gyral patterns, abnormal posterior fossae, megalencephaly, midline defects, fused thalami, amygdala and hippocampus malformations, and/or ventricular wall alterations [Barge-Schaapveld et al., 2011; Khonsari et al., 2012; Ludwig et al., 2012]. Further evaluation of the brain morphology in BBD–FGFR2 type may lead to greater insight into the role of FGFR2 signaling in abnormal and normal brain development and its connection with the development of the overlying calvaria.

It is unclear if there is a consistent relationship between genotype and phenotype in this disorder. Individuals with the p.Met391Arg mutation were all stillborn at or before 31 weeks gestation [Merrill et al., 2012]. Among the longer-term survivors, all showed heterozygosity

for a missense mutation at tyrosine residue 381. The three longest term survivors had the p.Tyr381Asp substitution but that mutation was also seen in two patients with neonatal death. Prematurity was common. The difference in outcome may reflect the extent of medical intervention but could be related to some variability in phenotypic expression. Regardless of the gestational age at the time of delivery, the radiographic phenotype is pathognomonic for the disorder and includes poor ossification of the calvarium, craniostenosis, small clavicles, bent appendicular bones, and angel shaped metacarpal/ metatarsal phalangeal bones. Based on the outcomes and findings in our longer-term survivors, the data suggests that the prognosis for this disorder is guarded.

All FGFRs have a similar protein structure comprised of three extracellular immunoglobulin-like domains, a single membrane-spanning segment, and a cytoplasmic tyrosine kinase domain. The transmembrane (TM) helix of FGFR2 allows for receptor integration into the lipid bilayer upon translation at the rough endoplasmic reticulum. The missense mutations observed in our series predict either substitution of a highly conserved hydrophobic residue with a positively (p.Met391Arg) or a negatively charged polar amino acid (p.Tyr381Asp or p.Tyr381Arg) in the TM helix. As previously reported [Merrill et al., 2012], levels of the fully glycosylated receptor were reduced in cultured cells from affected individuals, resulting in reduced FGFR2 levels at the membrane and enhanced FGFR2 localization to the nucleus. Cells inform us that patients with BBD-FGFR2 were shown to have reduced responsiveness to extracellular FGFs and increased responsiveness to intracellular FGFs [Merrill et al., 2012; Neben and Merrill, 2015]. While nuclear trafficking routes for FGFR2 are not yet completely understood, these results suggest altered receptor trafficking from the endoplasmic reticulum [Merrill et al., 2012].

The FGFR2 protein plays a critical role in the maturation and differentiation of osteoblasts. In developing bone, FGFR2 is predominantly localized to perichondrial and periosteal tissues. In cranial sutures, FGFR2 is mainly expressed in osteoprogenitor cells and differentiating osteoblasts. How these mutations affect the perichondrium and periosteum merits further investigation. Nevertheless, previous work shows that the mutations, by enhancing nuclear FGFR2 signaling, promote proliferation at the expense of differentiation in skeletal progenitor cells [Merrill et al., 2012; Neben and Merrill, 2015]. Our finding here of increased FGF23 serum levels in one of the longer-term survivors might shed further light on this mechanism. Recently, it was shown that nuclear FGFR1 promotes transcription of *FGF23* in osteoblasts to regulate phosphate homeostasis [Han et al., 2015]. Thus, it is possible that increased FGF23 levels in patients BBD-FGFR2 type results from enhanced activity of nuclear FGFR2 signaling. Beyond uncovering a role for FGFR2 in the nucleus of skeletal progenitor cells, the identification of this rare disorder, with a distinct clinical and radiographic phenotype, will likely continue to shed new insight on FGFR2 signaling by mechanisms that might not have been predicted from the outset and deepening our understanding of the interconnected pathways that regulate skeletogenesis.

Acknowledgments

References

Barge-Schaapveld DQ, Brooks AS, Lequin MH, van Spaendonk R, Vermeulen RJ, Cobben JM. Beare-Stevenson syndrome: Two Dutch patients with cerebral abnormalities. Pediatr Neurol. 2011; 44:03–307.

Han X, Xiao Z, Quarles LD. Membrane and integrative nuclear fibroblastic growth factor receptor (FGFR) regulation of FGF-23. J Biol Chem. 2015; 290:10447–10459. [PubMed: 25752607]

Handa A, Okajima Y, Izumi N, Yamanaka M, Kurihara Y. Bent bone dysplasia (BBD)-FGFR2 type: The radiologic manifestations in early gestation. Pediatr Radiol. 2016; 46:296–299. [PubMed: 26446305]

Hatch NE. FGF signaling in craniofacial biological control and pathological craniofacial development. Crit Rev Eukaryot Gene Expr. 2010; 20:295–311. [PubMed: 21395503]

Hollister DW, Klein SH, de Jager HJ, Lachman RS, Rimoin DL. Lacrimo-auriculo-dento-digital (LADD) syndrome. Birth Defects Orig Artic Ser. 1974; 10:153–166.

Khonsari RH, Delezoide AL, Kang W, Hebert JM, Bessieres B, Bodiguel V, Collet C, Legeai-Mallet L, Sharpe PT, Fallet-Bianco C. Central nervous system malformations and deformations in FGFR2-related craniosynostosis. Am J Med Genet Part A. 2012; 158A:2797–2806. [PubMed: 22987770]

Ludwig K, Salmaso R, Manara R, Cosmi E, Baldi M, Rugge M. Apert syndrome with fused thalami. Fetal Pediatr Pathol. 2012; 31:410–414. [PubMed: 22443264]

Merrill AE, Sarukhanov A, Krejci P, Idoni B, Camacho N, Estrada KD, Lyons KM, Deixler H, Robinson H, Chitayat D, Curry CJ, Lachman RS, Wilcox WR, Krakow D. Bent bone dysplasia-FGFR2 type, a distinct skeletal disorder, has deficient canonical FGF signaling. Am J Hum Genet. 2012; 90:550–557. [PubMed: 22387015]

Moosa S, Wollnik B. Altered FGF signalling in congenital craniofacial and skeldisorders. Semin Cell Dev Biol. pii: S1084-9521(15)30018–5.

Neben CL, Merrill AE. Signaling pathways in craniofacial development: Insights from rare skeletal disorders. Curr Top Dev Biol. 2015; 115:493–542. [PubMed: 26589936]

Rohmann E, Brunner HG, Kayserili H, Uyguner O, Nurnberg G, Lew ED, Dobbie A, Eswarakumar VP, Uzumcu A, Ulubil-Emeroglu M, Leroy JG, Li Y, Becker C, Lehnerdt K, Cremers CW, Yuksel-Apak M, Nurnberg P, Kubisch C, Schlessinger J, van Bokhoven H, Wollnik B. Mutations in different components of FGF signaling in LADD syndrome. Nat Genet. 2006; 38:414–417. [PubMed: 16501574]

Scott RH, Meaney C, Jenkins L, Calder A, Hurst JA. The postnatal features of bent bone dysplasia-FGFR2 type. Clin Dysmorphol. 2014; 23:8–11. [PubMed: 24300289]

Shams I, Rohmann E, Eswarakumar VP, Lew ED, Yuzawa S, Wollnik B, Schlessinger J, Lax I. Lacrimo-auriculo-dento-digital syndrome is caused by reduced activity of the fibroblast growth factor 10 (FGF10)-FGF receptor 2 signaling pathway. Mol Cell Biol. 2007; 27:6903–6912. [PubMed: 17682060]

Stichelbout M, Dieux-Coeslier A, Clouqueur E, Collet C, Petit F. A new case of bent bone dysplasia-FGFR2 type and review of the literature. Am J Med Genet Part A. 2016; 170:785–789. [PubMed: 26573129]

FIG. 1.
Facial photographs in three long-term survivors with bent bone dysplasia-FGFR2 type showing frontal bossing, severe midface hypoplasia, proptosis, small nose, and protruding tongue.
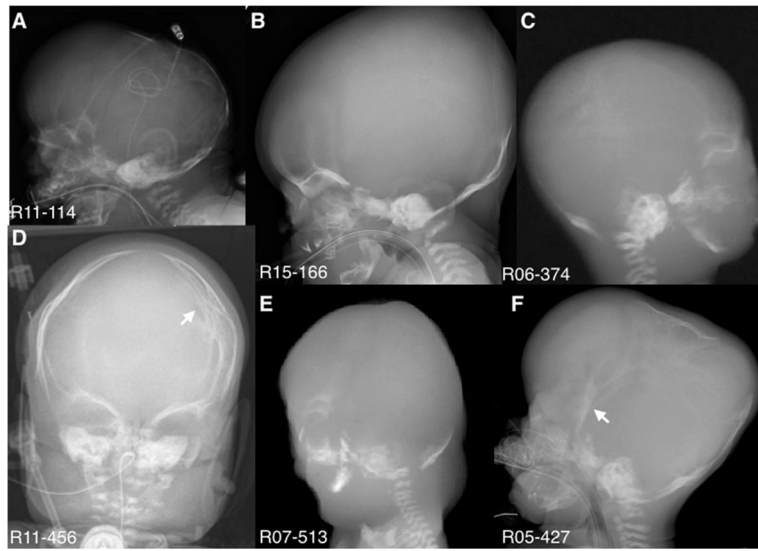
FIG. 2.
Lateral and Anterior/Posterior radiographs showing poorly mineralized calvaria and arrows point to areas of craniosynostosis. Small teeth are seen in B, C, E, and F.
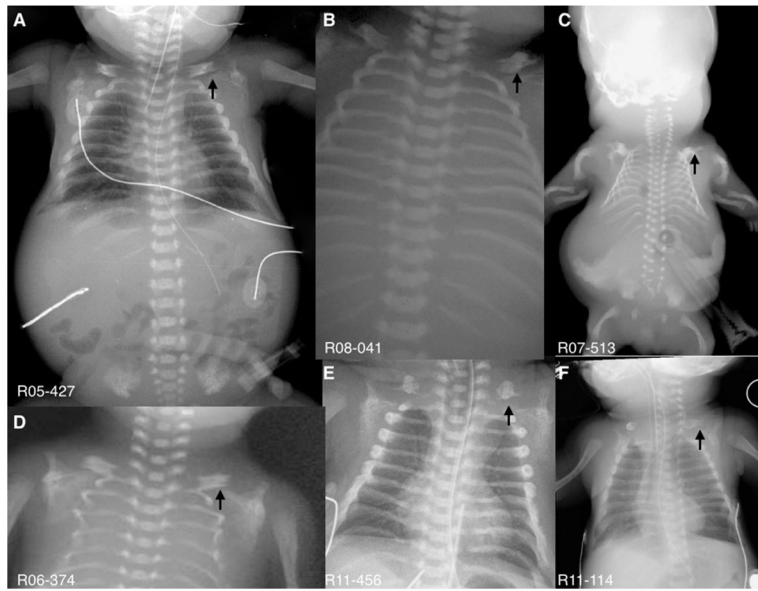
FIG. 3.
Series of radiographs from affected individuals showing the "moustached-shaped" small clavicles (arrows) and varying degrees of small chests with thin ribs (C and D).

FIG. 4.
Radiographs demonstrate the varying degree of bending in the appendicular skeleton (bent bones), particularly in the lower extremities. Bilateral fractures are seen in F.

FIG. 5.
Anterior/Posterior hand and feet radiographs showing the metacarpal, metatarsal, and phalangeal excrescences giving rise to the appearance of "Angel-shaped phalanges." Arrows point to "Angel-shaped" metacarpals, metatarsals, and/or phalanges. Boxed area in B shows expanded details of the "Angel-shaped" phalanges in E.

TABLE I

Clinical Features

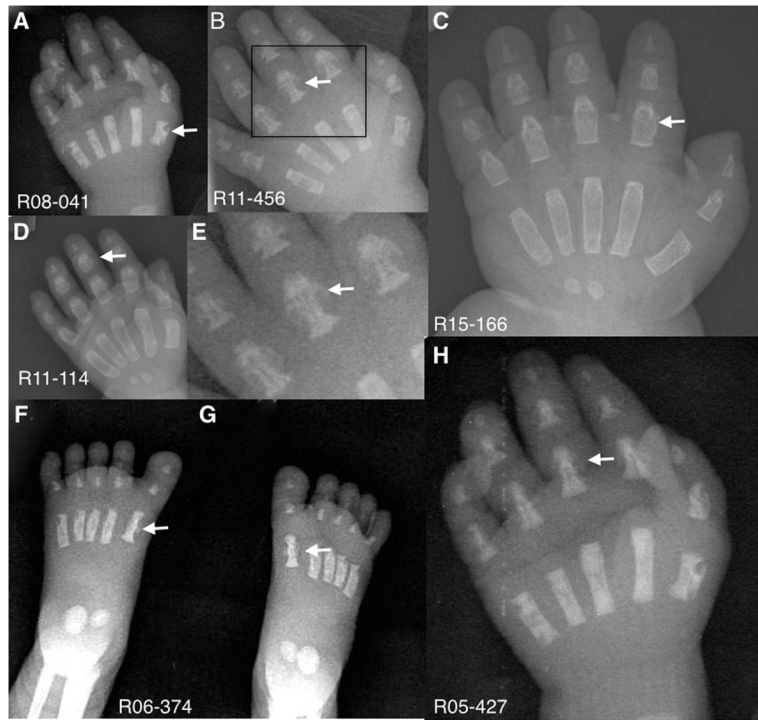| Case number	R96-252[a]	R07-401[a]	R08-041[a]	R05-427[a]	R89-051[b]	R06-374[b]	R11-456[b]	R15-166[b]	R11-114[b]	R07-513[b]	R16-035[b]
Sex	Male	Female	Female	Female	Male	Female	Male	Female	Female	Male	Female
Status	Stillborn at 29 weeks	Stillborn at 27 weeks	Stillborn at 31 weeks	Delivered at 32 weeks, neonatal death	Delivered at 38 weeks, neonatal death	Aborted fetus at 22 weeks	Delivered at 31 3/7 weeks, died at 3 months	Delivered at 35 weeks, alive at 5 months	Delivered at 30 5/7 weeks, alive at 13 months	Aborted fetus at 18 weeks	Delivered at 36 weeks, died at 4 days
FGFR2 mutation	c.1172T>G p.M391R[a] apparently de novo	c.1172T>G p.M391R[a] confirmed de novo	c.1172T>G p.M391R[a] confirmed de novo	c. p.Y381D[a] apparently de novo	c. p.Y381D apparently de novo	c. p.Y381D apparently de novo	c. p.Y381D apparently de novo	c. p.Y381D apparently de novo	c. p.Y381D confirmed de novo	N/A	N/A
Prenatal including ultrasound findings	Bowing of the femora and tibiae, short umbilical cord	Shortened appendicular bones, bent femora and tibiae, poor mineralization of the calvarium	Polyhydramnios, short bent femora	SGA, polyhydramnios, femoral mid-shaft angulation	Increased MSAFP, acrocephaly	Increased nuchal thickness	SGA, bowing of femora, tibiae, and fibulae, pyelectasis micrognathia	Abnormal second trimester screening, micrognathia, bell shaped chest, short extremities, polyhydramnios	Polyhydramnios, short umbilical cord	Multiple bent appendicular bones	Fetal distress, placenta abruption, short umbilical cord (12 inches)
Birth Length (cm) % for GA	33 (3rd %ile)	N/A	N/A	38 (<3rd %ile)	44.5 (<3rd %ile)	26 (N/A)	40 (25 %ile)	40.5 (<3rd %ile)	37 (15th %ile)	19 (N/A)	39 (<5th %ile)
Birth weight (g) % for GA	1,000 (10th %ile)	N/A	N/A	1,625 (25th %ile)	2,600 (25th %ile)	403 (N/A)	1,450 (25th %ile)	2,396 (50th %ile)	1,500 (50th %ile)	201 (N/A)	2,260 (25th %ile)
Head circumference (cm) % for GA	25.5 (10th %ile)	N/A	N/A	28.25 (25th %ile)	30.5 (<3rd %ile)	18 N/A	29 (50th %ile)	35 (>90th %ile)	28 (25th %ile)	15	32.5 cm (50th %ile)
Cranium	Large anterior fontanelle with open triangular metopic suture	Large anterior fontanelle	Cloverleaf shape	Large anterior fontanelle with open triangular metopic suture	Anterior fontanelle (4 × 8 cm), palpable synostoses of lambdoid and coronal sutures	Under-mineralized calvarial bones with widely patent sutures	Large anterior fontanelle with open triangular metopic suture	Cloverleaf shape, under-mineralized bone	Cloverleaf shape, large anterior fontanelle with open triangular metopic suture	Anterior fontanelle (4 × 3 cm), posterior fontanelle (3 × 2) cm	Multiple suture synostoses (except for lambdoid), frontal bossing, cloverleaf skull deformity, anterior and posterior fontanelles wide open
Eyes	Proptosis, hypertelorism	Periorbital swelling, hypertelorism, megalocornea clouding	Proptosis	Proptosis, hypertelorism, megalocornea	Proptosis	Proptosis, hypertelorism	Proptosis	Proptosis	Proptosis	Proptosis	Proptosis with periorbital swelling
Nose/philtrum	N/A	Short nose with depressed nasal bridge, long philtrum	Short nose with depressed nasal bridge, long philtrum	Short nose with depressed nasal bridge, long philtrum	Small upturned nose, left choanal atresia noted on CT scan	Small upturned nose, patent nares	Depressed nasal bridge, anteverted nares	Hypoplastic nasal bridge	Short nose with depressed nasal bridge	Short nose With Depressed nasal bridge	Short nose with depressed nasal bridge and long philtrum
Mouth	Protruding tongue, micrognathia, mandibular alveolar ridge cyst	Prominent upper labial frenulum, gum hypertrophy, micrognathia, prominent lips, large submucous cleft, perinatal teeth	N/A	Protruding tongue, micrognathia	–	Micrognathia, high arch palate, possible perinatal teeth erupting	Protruding tongue, micrognathia	Protuberant tongue, micrognathia	Protruding tongue, micrognathia	N/A	Protruding tongue, micrognathia, mandibular cyst
Ears	Normal	Low set ears, overfolded superior helix	Low set ears, overfolded superior helix	Normal	Posteriorly rotated	Normal	Slightly low set	Congenital stenosis of the auditory canal	Normal	Low set	Low set, abnormal shape
Renal/GU	Shawl scrotum, horseshoe kidney, unilateral cryptorchidism	Prominent clitoris and labia minora	Chloromegaly	None identified	Normal	Normal	None identified	Protuberant abdomen without organomegaly	Normal	Normal	Normal
Extremities	Brachydactyly, hypoplasia of the distal phalanges	Brachydactyly/edema, distal tapering of fingers	N/A	Brachydactyly, trident configuration of fingers, small nails	Limited extension at elbows, small nails	Bilateral varus deviation of the wrists	Normal	Brachydactyly, ligamentous laxity	Brachydactyly, trident configuration of fingers	Normal	Brachydactyly, trident configuration of fingers
Other clinical features	Small chest, hypoplastic lungs, Meckel's diverticulum	Hypertrichosis	Hepatosplenomegaly with extramedullary hematopoiesis	Small chest	Unilateral choanal atresia		Small chest, hypertrichosis	Narrow chest, patent foramen ovale, tracheostomy placed, respiratory compromise, decreased muscle mass, hypotonia, slow transit constipation, G-tube placed FGF23 278 (NL. <= 230)	Arnold Chiari malformation, hydrocephalus, compression of the superior sagittal sinus, bilateral medullary nephrocalcinosis without hypercalciuria, laryngeal edema, tracheostomy, and G-tube placed	Abdominal ascites, cecum, and appendix in the midline	Extensive extramedullary hematopoiesis, replacement of a large portion of the bone marrow spaces with fibrous dysplasia-like lesions, pulmonary arterial hypoplasia

N/A, not available; %, percentile; GA, gestational age; g, grams; cm, centimeters.

[a] Previously reported [Merrill et al., 2012].

[b] Newly reported.

TABLE II

Major Radiological Features

Case number	R96-252[a]	R07-401[a]	R08-041[a]	R05-427[a]	R89-051[b]	R06-374[b]	R11-456[b]	R15-166[b]	R11-114[b]	R07-513[b]	R16-035[b]
Age of at time of radiographs	28 wk	27 wk	31 wk	22 wk	38 wk	22 wk	1 month	35 wk	30 wk	18 wk	36 wk
Mustache-shaped clavicles	+	+	+	+	+	+	+	+	+	+	+
Hands angel-shaped phalanges/metacarpals	+	+	+	NA	+	+	+	+	+	NA	+
Feet angel-shaped phalanges/metatarsals	+	+	+	NA	NA	+	+	+	NA	NA	+
Bent femora	+	+	+	+	+	+	+	+	+	+	+
Craniosynostosis	+	NA	+	+	+	+	+	−	+	+	+
Decreased skull ossification	−	NA	+	+	+	+	−	+	+	+	+
Abnormally formed teeth	+	NA	+	+	+	+	NA	−	3	NA	+

NA, not available; wk, weeks.

[a]Previously published [Merrill et al., 2012].

[b]Newly described cases.